IEEE Access
Multidisciplinary | Rapid Review | Open Access Journal

Received June 15, 2018, accepted July 29, 2018, date of publication August 1, 2018, date of current version August 28, 2018.

Digital Object Identifier 10.1109/ACCESS.2018.2861885

Model-Guided Data-Driven Decentralized Control for Magnetic Levitation Systems

QIANG CHEN[1], YING TAN[2], (Senior Member, IEEE), JIE LI[1], DENNY OETOMO[2], (Senior Member, IEEE), AND IVEN MAREELS[2], (Fellow, IEEE)

[1]College of Intelligent Science, National University of Defense Technology, Changsha 410073, China
[2]Melbourne School of Engineering, The University of Melbourne, Melbourne, VIC 3010, Australia

Corresponding author: Qiang Chen (Chen_NUDT@outlook.com)

This work was supported in part by the National Key Research and Development Program of China under Grant 2016YFB1200600, in part by the Research Plan Program of the National University of Defense Technology under Grant 2K16-02-02, and in part by the Opening Foundation of the State Key Laboratory of Functional Materials for Informatics under Grant SKL-2017-07.

ABSTRACT This paper presents a half bogie model of magnetic levitation systems, which can capture the mechanical coupling between two suspension points. Based on the half bogie model, a model-guided state feedback controller is designed to stabilize the nominal model. A new extended state observer using measured data is proposed to estimate the unknown system state as well as the modeling uncertainties, disturbances, and coupling. This leads to an active disturbance rejection controller that can cancel the effect of unknown disturbances. By incorporating model-guided state feedback controller and the data-driven active disturbance rejection controller with an appropriate tuning of parameters, the closed loop system can track the desired gap up to any given accuracy. Simulation and experimental results demonstrate the effectiveness of the proposed method.

INDEX TERMS Magnetic levitation systems, model-guided data-driven control, extended state observer.

I. INTRODUCTION

Magnetic Levitation (Maglev) trains use electromagnetic forces to stably levitate the trains above the track [1]. Compared with traditional wheel rail trains, Maglev trains have many advantages such as safety, comfort, low noise, small turning radius, strong climbing ability [2]. ElectroMagnetic Suspension (EMS) structure is one of the major suspension modes and has been applied in some popular Maglev trains, such as Transrapid, HSST and CMS [3]–[5]. The schematic diagram is shown in Fig. 1.

As any EMS system is open loop unstable, the control design, which aims at maintaining the desired gap, plays an important role. Regulation of EMS Maglev train with the desired performance, in terms of transient response and steady-state error, is quite challenging. There are two major reasons for undesired performance.

a A precise model for EMS systems is very hard to obtain due to highly nonlinear behaviours coming from the structure of the system with its magnetic field distribution, quality of rails, complex motion of trains, the existence of various uncertainties and disturbances due to weather conditions, driving conditions and so on.

b The structure of Maglev system and its controllers would limit the closed loop performance. For example, bogies based train structure [6], [7] and decentralized control structure [8], [9] have been widely used in Maglev trains due to its simplicity in design and implementation. The diagram of decentralized control structure is presented in Fig. 2. The decentralized control structure implies that each suspension point has its own control loop and typically all suspension points share the same identical control structure and parameters.

This requires that the parameters of decentralized control has to be designed with very robust properties to ensure that the worst case among all suspension points can work. That is very challenging.

This paper aims at addressing this challenging problem by designing a robust controller for a half bogie with a decentralized controller structure as shown in Fig. 2.

A simple way to control such a system with the consideration of decentralized structure is to use two identical PID controllers, by trial and error method. A typical performance of such a decentralized PID control is shown in Fig. 3.

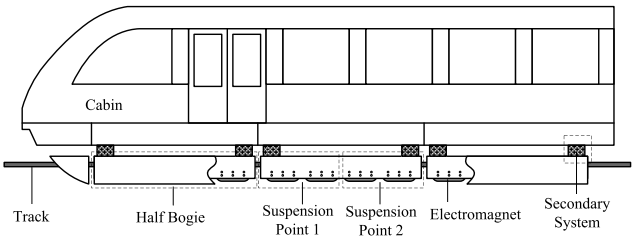

FIGURE 1. Schematic diagram of EMS type Maglev train.

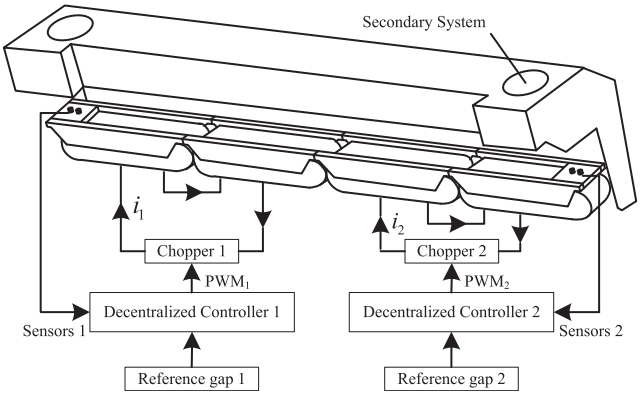

FIGURE 2. Decentralized control system for a half bogie.

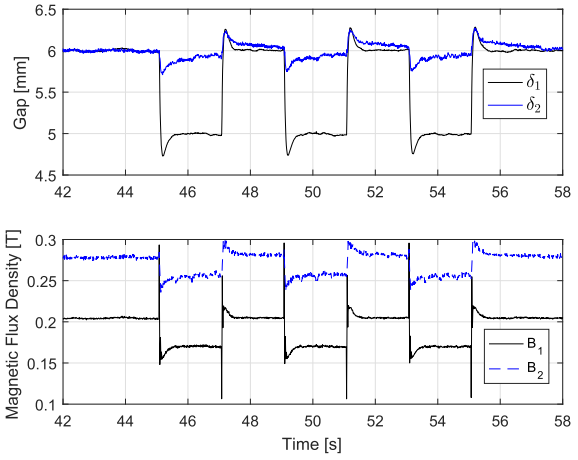

FIGURE 3. The performance of decentralized PID controller.

From these results, it can be seen that the decentralized PID controllers work fine. Each suspension point can be stably suspended in the setting gap ($6mm$). Fig. 3 also shows that with the same initial condition, the same set-point, the same PID parameters, the transient response and the steady state response of Suspension Point 1 (SP1) and Suspension Point 2 (SP2) are quite different. The possible reasons are weight distribution of the half bogie is uneven and the two suspension points are not exactly parallel to the track.

Moreover, it is observed that the steady-state of SP2 is around $0.25mm$ when the gap of SP1 is set to track a square wave signal with period $1mm$ to simulate external disturbances. This indicates that the mechanical coupling does exist.

It is well-known that PID controller design for nonlinear systems is a model-free method. Trial and error method is the only choice. Without the model, the tuning of controller parameters becomes challenging.

Other than model-free PID controllers, extended state observer (ESO) [10]–[13] and active disturbance rejection controller (ADRC) can be treated as another model-free control design. The idea of ESO is to use less model information to estimate the state of the system as well as unknown lumped uncertainties including modelling uncertainties and disturbances. More precisely, when the model of engineering system has some structure and the lumped uncertainties are treated as the ''black-box'', the ESO can estimate these lumped uncertainties using measurements. In general, the ESO is a high gain observer, which can estimate relatively slow time-varying unknown disturbances [14]–[18]. Once the lumped uncertainties are identified, the ADRC [19]–[23] can cancel the influence of uncertainties and achieve robust stability.

Of course, there are other model-free methods that can be implemented on-line, such as adaptive fuzzy control and adaptive neural network [24]–[26]. As many weights are needed to tune on-line, it requires extensive computational resources and sufficient rich persistent excitation signals to ensure the convergence. These two conditions are not easy to be implemented on Maglev system with given performance requirement and computation powers.

When the system is repetitive over a finite time interval, iterative learning control (ILC) law can be used as a model-free or data-driven technique to ''learn'' from the past experience as in [27]. However, the Maglev system is not repetitive in finite time, though it might be repetitive in space. Hence the standard ILC technique cannot be directly applied.

On the other hand, based on the limited model information, some model-based controllers have been proposed to design the decentralized controllers for EMS systems with the aim to improve the robustness of the closed loop in the presence of modeling uncertainties and disturbances. For example, disturbance observers have been used in the combination of model-based control design, see [28]–[30] and references there in. When the uncertainties are matched, sliding-mode control (SMC) can use high-gain controllers to cancel the effect of the worst case disturbance as indicated in [31]–[34]. The high-gain nature of SMC usually leads to high-frequency chattering, which is not preferred in Maglev systems. Other techniques include estimating and rejecting the disturbances using internal model principal (IMP) when the disturbance model is known [35].

Usually, neither model-based design nor model-free design can work well for complicated engineering systems such as EMS. This work exploits the model of a half bogie from physical principles of EMS Maglev systems. The control input consists of two parts. The first one is a standard

feedback controller, which aims at stabilizing the system using the information of the model. By estimating uncertainties and disturbances on-line, the second controller tries to cancel the effect of uncertainties and disturbances, so that the stability of the closed loop system is ensured. It is worthwhile to highlight that as only the gap information is measured from sensor, an observer is design to estimate the state, which will be used in the first controller, as well as the unknown modelling uncertainties and disturbances.

This technique is a kind of model-guided data-driven controller as both the knowledge of the model and measured data are used. It is shown in the main result (Theorem 1) that by tuning the parameters of the proposed model-guided data-driven controller properly, the stability of the closed loop can be guaranteed with the desired tracking performance. In other words, for any given domain of attraction and the ultimate bound, it is possible to find the suitable parameters to ensure that any trajectory starting within the given the domain of attraction will converge to the given ultimate bound.

The proposed model-guided data-driven method is different from the well-known model-free technique which is a combination of ESO and ADRC [19], [22]. In the proposed control methods, two controllers are used. The first controller is designed based on the nominal model. The role is to ensure the boundedness of the trajectories under mild assumption. The second control is designed with the help of ESO. The role of it is to cancel the influence of lumped uncertainties once the ESO estimate them. It is also noted that since only part of the state is measurable, the role of ESO is to estimate the unknown state as well as the unknown uncertainties. It is noted that since the state is uniformly bounded due to the existence of the first controller, the design of ESO and the second control becomes relatively easier.

The reminder of the paper is organized as follows. Modelling of the half bogie with the consideration of mechanic coupling is presented in Section 2. Section 3 presents a general problem formulation, the model-guided data-driven control design and stability analysis. Simulations and experimental results shown in Section 4, followed by conclusion in Section 5.

The following notations are used in this paper. The set of real numbers is denoted as $\mathcal{R}$. For any $\boldsymbol{x} \in \mathcal{R}^n$, $|\boldsymbol{x}| = \sqrt{\boldsymbol{x}^t\boldsymbol{x}}$. For any $\Delta > 0$, the set $\Delta_{\boldsymbol{x}}$ is defined as $\Delta_{\boldsymbol{x}} = \{\boldsymbol{x} \in \mathcal{R}^n \,||\boldsymbol{x}| \leq \Delta|\,.\}$. The set $\mathcal{L}_\infty$ denotes the set of all bounded signals such that for any $\boldsymbol{u}(\cdot) \in \mathcal{L}_\infty$, $\text{esssup}_{t\geq 0}\,|\boldsymbol{u}(t)| < \infty$ with its norm is defined as $\|\boldsymbol{u}\|_\infty := \text{esssup}_{t\geq 0}\,|\boldsymbol{u}(t)|$. The set $\mathcal{C}[0,\infty)$ denotes the set of all continuous signals defined on the interval $[0,\infty)$.

A continuous function $\gamma : \mathcal{R}_{\geq 0} \to \mathcal{R}_{\geq 0}$ belongs to class-$\mathcal{K}$ if it is strictly increasing and $\gamma(0) = 0$. It is of class- $\mathcal{K}_\infty$ if it belongs to class-$\mathcal{K}$ and is unbounded. A function $\beta : \mathcal{R}_{\geq 0} \times \mathcal{R}_{\geq 0} \to \mathcal{R}_{\geq 0}$ is of class-$\mathcal{KL}$ if $\beta(\cdot, t)$ belongs to class-$\mathcal{K}$ for each $t \geq 0$ and $\beta(s;\cdot)$ is decreasing to zero for each $s > 0$ [36].

II. MODELS FOR A HALF BOGIE

In order to understand the characteristics of the Maglev system, a first-principle based model is needed. Compared with traditional current feedback, flux feedback [37]–[39] for EMS has some advantages. For example, the model of suspension will be less nonlinear, making it relatively easier to design a model-guided controller.

In order to generate sufficient large magnetic force as soon as possible to balance the gravity, a cascade controller, which consists of the fast inner flux loop and the slow outer gap loop, has been widely used [40], [41]. The outer loop regulates the gap. The inner loop drives the magnetic flux density response quickly to desired reference from the gap loop to generate enough magnetic force. The inner loop is an electrical system. It uses the PWM signal as a control input to generate current in EMS to form the magnetic field. It can be modeled as a simple first order system. A standard proportional control can work [33],[36]. The outer loop is a mechanical system, which is quite hard to model due to the existence of disturbances. In this paper, the design of the outer loop is mainly considered.

A schematic diagram of a half bogie is represented in Fig. 4. Here m is the mass of the half bogie, l is the length of the half bogie, c is the gap between the center of the half bogie and the track, θ is the pitching angle of the half bogie, δ_1 and δ_2 are the gap of SP1 and SP2 measured by the gap sensors. F_1 and F_2 are the equivalent electromagnetic force of SP1 and SP2, H_1 and H_2 are the equivalent force exerted by the cabin on SP1 and SP2 through the secondary system.

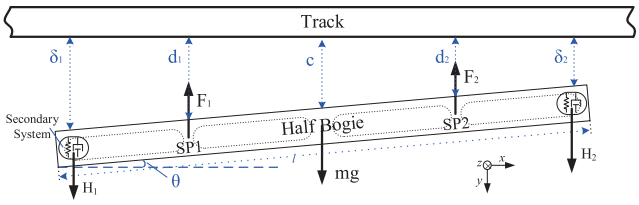

FIGURE 4. The schematic diagram of a half bogie.

In order to design a model-guided controller, a half bogie model is needed. The following standard assumptions are used to simplify the modeling procedure.

1) Leakage flux can be ignored.
2) The magnetic saturation can be ignored.
3) Magneto-resistance in core and track can be ignored.
4) The motion of rolling and yawing between electromagnets and the track is negligible.
5) The elastic vibration or dynamic deformation of the track is negligible.
6) The half bogie structure is simplified as a uniform mass rod, the gravity center and geometric center coincide.
7) The electromagnetic force of each suspension point is equivalent to a concentrating force.

With these assumptions, the mechanical and kinetic equations of the half bogie can be described as:

$$m\ddot{c} = mg + H_1 + H_2 - F_1 - F_2 \tag{1}$$

$$J\ddot{\theta} = F_2 \cdot \frac{l}{4} \cdot cos(\theta) - F_1 \cdot \frac{l}{4} \cdot cos(\theta) + H_1 \cdot \frac{l}{2} \cdot cos(\theta) - H_2 \cdot \frac{l}{2} \cdot cos(\theta), \tag{2}$$

where J is the rotary inertia of half bogie along z-axis.

The geometric relationships provide the following relations:

$$c = \frac{1}{2}\delta_1 + \frac{1}{2}\delta_2 \tag{3}$$

$$d_1 = \frac{3}{4}\delta_1 + \frac{1}{4}\delta_2 \tag{4}$$

$$d_2 = \frac{1}{4}\delta_1 + \frac{3}{4}\delta_2. \tag{5}$$

As the gap is very small relative to the length of the half bogie, pitch angle is very small. That is,

$$\theta \approx sin[\theta] = \frac{\delta_1 - \delta_2(t)}{l} \tag{6}$$

$$cos(\theta) \approx 1. \tag{7}$$

The electromagnetic force of each suspension point can be described as:

$$F_1 = \frac{2A}{\mu_0}B_1^2 \tag{8}$$

$$F_2 = \frac{2A}{\mu_0}B_2^2, \tag{9}$$

where μ_0 is permeability of vacuum, A is the effective area of per electromagnet, B_1 and B_2 are magnetic flux density of SP1 and SP2 respectively. Magnetic flux density can be calculated by the relationship [38]:

$$B_1 = \frac{\mu_0 N i_1}{2d_1} \tag{10}$$

$$B_2 = \frac{\mu_0 N i_2}{2d_2}, \tag{11}$$

where N is the number of coil of per electromagnet, i_1 and i_2 are current in electromagnets of SP1 and SP2 respectively..

H_1 and H_2 of the secondary system can be described as [28], [39]

$$H_1 = M_1 g - k_s(\delta_1 - \delta_{c1} - \Delta_{ce1}) - c_s(\dot{\delta}_1 - \dot{\delta}_{c1}) \tag{12}$$

$$H_2 = M_2 g - k_s(\delta_2 - \delta_{c2} - \Delta_{ce2}) - c_s(\dot{\delta}_2 - \dot{\delta}_{c2}), \tag{13}$$

where $M_1 g$ and $M_2 g$ are the gravity applied by the cabin to the SP1 and SP2 through the secondary system. Here δ_{c1} and δ_{c2} are the position of the cabin relative to SP1 and SP2 respectively. Variables k_s and c_s are the elastic coefficient and damping coefficient of the secondary system respectively. Notions of Δ_{ce1} and Δ_{ce1} are the initial deformation of the secondary system above SP1 and SP2.

The load of actual system is usually varied, but a nominal value M exists as

$$M_1 = M_2 = \frac{M}{2}. \tag{14}$$

Moreover, it is denoted

$$N_1 = g(1 + \frac{M}{m}) + k_x k_s(\delta_{c1} + \Delta_{ce1}) + k_x c_s(\dot{\delta}_{c1}) + k_z k_s(\delta_{c2} + \Delta_{ce2}) + k_z c_s(\dot{\delta}_{c2}) \tag{15}$$

$$N_2 = g(1 + \frac{M}{m}) + k_z k_s(\delta_{c1} + \Delta_{ce1}) + k_z c_s(\dot{\delta}_{c1}) + k_x k_s(\delta_{c2} + \Delta_{ce2}) + k_x c_s(\dot{\delta}_{c2}), \tag{16}$$

where

$$k_x = \frac{1}{m} + \frac{l^2}{4J}, \tag{17}$$

$$k_z = \frac{1}{m} - \frac{l^2}{4J}. \tag{18}$$

With the consideration of all relationships mentioned and disturbances (w_1 and w_2), the following state-space representation of the half bogie model is obtained:

$$\dot{\boldsymbol{s}} = \begin{bmatrix} 0 \\ N_1 \\ 0 \\ N_2 \end{bmatrix} + \begin{bmatrix} 0 & 1 & 0 & 0 \\ -k_x k_s & -k_x c_s & -k_z k_s & -k_z c_s \\ 0 & 0 & 0 & 1 \\ -k_z k_s & -k_z c_s & -k_x k_s & -k_x c_s \end{bmatrix} \boldsymbol{s} + \begin{bmatrix} 0 & 0 \\ -\frac{2A}{m\mu_0} - \frac{Al^2}{4J\mu_0} & -\frac{2A}{m\mu_0} + \frac{Al^2}{4J\mu_0} \\ 0 & 0 \\ -\frac{2A}{m\mu_0} + \frac{Al^2}{4J\mu_0} & -\frac{2A}{m\mu_0} - \frac{Al^2}{4J\mu_0} \end{bmatrix} \boldsymbol{u} + \boldsymbol{w} \tag{19}$$

$$\boldsymbol{y} = \begin{bmatrix} 1 & 0 & 0 & 0 \\ 0 & 0 & 1 & 0 \end{bmatrix} \boldsymbol{s}, \tag{20}$$

where

$$\boldsymbol{s} = [\, x_1 \quad x_2 \quad z_1 \quad z_2 \,]^T = [\, \delta_1 \quad \dot{\delta}_1 \quad \delta_2 \quad \dot{\delta}_2 \,]^T \tag{21}$$

$$\boldsymbol{u} = [\, u_1 \quad u_2 \,]^T = [\, B_1^2 \quad B_2^2 \,]^T \tag{22}$$

$$\boldsymbol{y} = [\, y_1 \quad y_2 \,]^T = [\, x_1 \quad z_1 \,]^T \tag{23}$$

$$\boldsymbol{w} = [\, 0 \quad w_1 \quad 0 \quad w_2 \,]^T \tag{24}$$

A half model is thus obtained, it can be seen that the states of each suspension point are affected by the other suspension point, there is a coupling effect between suspending points.

Remark 1: Although this model is able to capture the mechanical coupling in a half bogie, it is still too simple to fully describe the behaviors of the half bogie due to the fact that some assumption cannot hold. Moreover, disturbances always exist. Even though better models including the other direction motion (heave, slip, roll, pitch, and yaw) [42], [43] are available, these models are still, might be better, approximations of the Maglev system, which consists of the dynamics of the track, the secondary system and so on [39], [44]. Each component is highly nonlinear. Thus it is very challenging to build a relatively accurate model so that mature model-based control algorithms are applicable. ◦

Considering the complexity of the system including model uncertainty, external disturbance and so on, a general model can be written as

$$\begin{cases} \dot{x}_1 = x_2 \\ \dot{x}_2 = G_1(x_1, x_2) + bu_1 + f_1(t, x_1, x_2, z_1, z_2, w_1, u_1, u_2) \\ y_1 = x_1 \\ \dot{z}_1 = z_2 \\ \dot{z}_2 = G_2(z_1, z_2) + bu_2 + f_2(t, x_1, x_2, z_1, z_2, w_2, u_1, u_2) \\ y_2 = z_1 \end{cases} \tag{25}$$

where $G_1(\cdot,\cdot)$ and $G_1(\cdot,\cdot)$ are the known part of the system model. In Maglev system, $G_1(\cdot,\cdot) = G_2(\cdot,\cdot) = G_0 = \frac{g}{2}(1 + \frac{M}{m})$, while $f_1 : [t_0, \infty) \times \mathcal{R} \times \mathcal{R} \times \mathcal{R} \times \mathcal{R} \times \mathcal{R} \times \mathcal{R} \times \mathcal{R} \times \mathcal{R} \to \mathcal{R}$ and $f_2 : [t_0, \infty) \times \mathcal{R} \times \mathcal{R} \times \mathcal{R} \times \mathcal{R} \times \mathcal{R} \times \mathcal{R} \times \mathcal{R} \times \mathcal{R} \to \mathcal{R}$ are unknown but continuous function. Here b is a known non-zero constant, it can be chosen as $b = -\frac{2A}{m\mu_0} - \frac{Al^2}{4J\mu_0}$. The initial state is denoted as

$$\begin{bmatrix} x_1(t_0) \\ x_2(t_0) \\ z_1(t_0) \\ z_2(t_0)) \end{bmatrix} = \boldsymbol{s}_0 \in \mathcal{R}^4, \quad \forall t \geq t_0 \geq 0. \tag{26}$$

For any given $\boldsymbol{u} \in \mathcal{L}_\infty$, the solutions of (25) are denoted as $\boldsymbol{s}(t; t_0, s_0, u(\cdot))$.

This paper uses a new design strategy. That is, a stabilizing controller is used to stabilize the known part of the system from modeling. The robustness of this stabilizing controller (model-guided) will ensure the boundedness of the trajectories. Once the trajectories are bounded, it is possible to design an ESO to estimate the unknown part including various modeling uncertainties, disturbances as well as coupling among two points. Then an extra ADRC will only cancel the effect of unknown part.

III. MODEL-GUIDED DATA-DRIVEN DECENTRALIZED CONTROL DESIGN

For the system (25), two extended states x_3 and z_3 which represent unmodeled uncertainties and external disturbances including the coupling can be defined as

$$x_3 = f_1(t, x_1, x_2, z_1, z_2, w_1, u_1, u_2), \tag{27}$$
$$z_3 = f_2(t, x_1, x_2, z_1, z_2, w_2, u_1, u_2), \tag{28}$$

In the presence of an extended state, the system (25) can be presented as Σ_1 and Σ_2 which are de-coupled and identical.

$$\Sigma_1 : \begin{cases} \dot{x}_1 = x_2 \\ \dot{x}_2 = x_3 + bu_1 + G_0 \\ y_1 = x_1 \end{cases} \tag{29}$$

$$\Sigma_2 : \begin{cases} \dot{z}_1 = z_2 \\ \dot{z}_2 = z_3 + bu_2 + G_0 \\ y_2 = z_1. \end{cases} \tag{30}$$

For simplicity, it is denoted that

$$\begin{aligned} \dot{x}_3 &= \frac{\partial f_1}{\partial t} + \frac{\partial f_1}{\partial x_1}\dot{x}_1 + \frac{\partial f_1}{\partial x_2}\dot{x}_2 + \frac{\partial f_1}{\partial z_1}\dot{z}_1 + \frac{\partial f_1}{\partial z_2}\dot{z}_2 \\ &\quad + \frac{\partial f_1}{\partial w_1}\dot{w}_1 + \frac{\partial f_1}{\partial u_1}\dot{u}_1 + \frac{\partial f_1}{\partial u_2}\dot{u}_2 - b\dot{u}_1 \\ &= f_{o,1}(t, x_1, x_2, z_1, z_2, w_1, u_1, u_2). \end{aligned} \tag{31}$$

$$\begin{aligned} \dot{z}_3 &= \frac{\partial f_2}{\partial t} + \frac{\partial f_2}{\partial x_1}\dot{x}_1 + \frac{\partial f_2}{\partial x_2}\dot{x}_2 + \frac{\partial f_2}{\partial z_1}\dot{z}_1 + \frac{\partial f_2}{\partial z_2}\dot{z}_2 \\ &\quad + \frac{\partial f_2}{\partial w_2}\dot{w}_2 + \frac{\partial f_2}{\partial u_1}\dot{u}_1 + \frac{\partial f_2}{\partial u_2}\dot{u}_2 - b\dot{u}_2 \\ &= f_{o,2}(t, x_1, x_2, z_1, z_2, w_2, u_1, u_2). \end{aligned} \tag{32}$$

The control objective is to design a control input $\boldsymbol{u}$ such that the output $\boldsymbol{y}$ is able to track the desired set-point (r_1, r_2) in the presence of modeling uncertainties, disturbances and coupling.

It is noted that two subsystems are very identical, we only focus on the design of the first subsystem. The similar analysis is applied to the second subsystem.

A. MODEL-GUIDED CONTROL DESIGN

Firstly, considering the system Σ_1 (29), which contains known parts $G_1(\cdot,\cdot)$ and unknown part $f_1(\cdot,\cdot,\cdot,\cdot,\cdot,\cdot,\cdot,\cdot)$ (or the extended state x_3)

If without considering the unknown uncertainties and disturbances, assuming $f_1(\cdot,\cdot,\cdot,\cdot,\cdot,\cdot,\cdot,\cdot) = 0$, the system Σ_1 will be

$$\Sigma_{1,m} : \begin{cases} \dot{x}_1 = x_2 \\ \dot{x}_2 = bu_1 + G_0 \\ y_1 = x_1. \end{cases} \tag{33}$$

If the state is measurable, the following model guided controller is proposed

$$u_{1,m} = \frac{1}{b}[-G_0 - k_1(x_1 - r_1) - k_2 x_2]. \tag{34}$$

If constants k_1 and k_2 are selected such that the matrix $A := \begin{bmatrix} 0 & 1 \\ -k_1 & -k_2 \end{bmatrix}$ is a Hurwitz, this controller can regulate the model (33). However, the state x_2 cannot be measured directly. An observer is needed.

Remark 2: If A is Hurwitz, for any symmetric positive definite matrix $Q \in \mathcal{R}^{2\times 2}$, there exists a symmetric positive definite matrix $P \in \mathcal{R}^{2\times 2}$ such that $A^T P + PA = -Q$. ∘

With $u_{1,m}$, the nominal system $\Sigma_{1,m}(33)$ will be stable. Due to the existence of uncertainties, disturbances and the coupling, this control law is not good enough. If the state x_3 can be estimated, then the following ADRC control law can work

$$u_{1,d} = -\frac{x_3}{b}. \tag{35}$$

If an appropriate observer can estimate x_2 and x_3 by $\hat{x}_2$ and $\hat{x}_3$ from measured data, this leads to the following Model-guided Data-driven Decentralized Controller:

$$u_{1,md} = \frac{1}{b}[-G_0 - k_1(x_1 - r_1) - k_2\hat{x}_2 - \hat{x}_3] \tag{36}$$

For simplicity, the following notations are considered: $e_1 = x_1 - r_1$, $\boldsymbol{x} = \begin{bmatrix} x_1 & x_2 & x_3 \end{bmatrix}^T$, $\hat{\boldsymbol{x}} = \begin{bmatrix} \hat{x}_1 & \hat{x}_2 & \hat{x}_3 \end{bmatrix}^T$ and $\tilde{\boldsymbol{x}} = \begin{bmatrix} \tilde{x}_1 & \tilde{x}_2 & \tilde{x}_3 \end{bmatrix}^T$. $\hat{x}_1$, $\hat{x}_2$ and $\hat{x}_3$ are the estimation of x_1, x_2 and x_3, $\tilde{x}_1 = y_1 - \hat{x}_1$, $\tilde{x}_2 = x_2 - \hat{x}_2$, and $\tilde{x}_3 = x_3 - \hat{x}_3$.

In order to make sure that the control input u_1 is able to be implemented, the following assumption is needed:

Assumption 1: For any given positive pair (Δ_s, Δ_u), any G_0 and r_1, there exists a positive pair (k_1^*, k_2^*) such that for any $\boldsymbol{x} \in \Delta_s$ and $\hat{\boldsymbol{x}} \in \Delta_s$, for any $|k_1| \leq k_1^*$ and $|k_2| \leq k_2^*$, $u_{1,md} \in \Delta_u$.

Remark 3: This assumption shows that it is possible to choose an appropriate bound for k_1 and k_2 for (36) so that if the state and estimated state are bounded, the control input will be bounded by a given value. This assumption plays an important role in the closed loop stability analysis. It indicates that the feedback gain cannot be arbitrarily designed even though the system (25) is completely controllable. The most difficult of stability analysis in this structure is the coupling between the controller and the observer. As the system is not linear, the standard Separation Principle for linear systems cannot be applied. Thus the observer and control law will affect each other, leading to possibly unstable performance. Hence the focus of this paper is to show semi-global performance, in which both the system and the observer work in a given compact set. Without fixing a compact set, the proposed method cannot work. ∘

Furthermore, in most applications, the rate of control input is bounded. Then the following filtered control input can be applied to the system:

$$\dot{u}_1 = \tau_1(-u_1 + u_{1,md}), \tag{37}$$

where τ_1 is the frequency of the low-pass filter.

It is also assumed that the low-pass filter is well-designed.

Assumption 2: Let $\epsilon_0 \geq 0$ be given, there exists $\tau_{1,a} > 0$ such that for any $\tau_1 \geq \tau_{1,a}$, $\operatorname{esssup}_{t\geq 0} |u_1 - u_{1,dm}| \leq \epsilon_0$. Moreover, for any given $\tau_{1,b}$ such that for any $\tau_1 \in (0, \tau_{1,b}]$, there exists a positive constant Δ_{du} such that $\operatorname{esssup}_{t\geq 0} |\dot{u}_1| \leq \Delta_{du}$.

Remark 4: This assumption indicates that the cut-off frequency of the filter cannot be too small, leading to a large ϵ_0. Moreover, the cut-off frequency cannot be too large, leading to a large Δ_{du}. By fixed ϵ_0, and selecting $\tau_{1,b} > \tau_{1,a}$, for any $\tau_1 \in [\tau_{1,a}, \tau_{1,b}]$, there exists Δ_{du} such that $\operatorname{esssup}_{t\geq 0} |u_1 - u_{1,md}| \leq \epsilon_0$ and $\operatorname{esssup}_{t\geq 0} |\dot{u}_1| \leq \Delta_{du}$. If $|\dot{u}_{1,md}|$ is small, the filter is not needed. Consequently, it has $\epsilon_0 = 0$ and $u_1 = u_{1,dm}$. ∘

These two assumptions play an important role in the design of ESO as well as the stability analysis. These two assumptions indicate that other than only providing stability for known part of the system (25), the control input u_1 needs to be bounded with a bounded derivative.

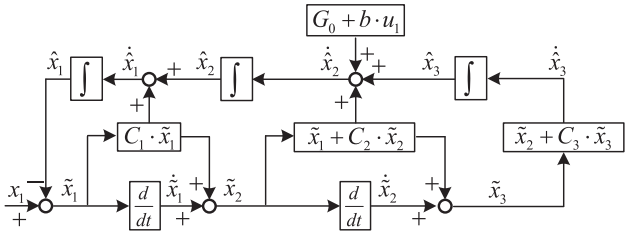

FIGURE 5. Block diagram of ESO.

B. THE DESIGN OF ESO

Note that in order to estimate the state signals of Σ_1 (29) and Σ_2 (30), the following assumptions are needed.

Assumption 3: The disturbances are bounded and slowly time-varying, i.e. there exists a positive constant pair (Δ_w, Δ_{dw}) such that $\|\boldsymbol{w}\|_\infty \leq \Delta_w$ and $\|\dot{\boldsymbol{w}}\|_\infty \leq \Delta_{dw}$.

Assumption 4: For a given Δ_s, Δ_u, Δ_{du}, Δ_w, and Δ_{dw}, there exist positive constants L_1, L_2, L_3, L_4, L_5, L_6, L_7, L_8 and L_9, M_1, M_2, M_3, M_4, M_5, M_6, M_7, M_8 and M_9 such that $|f_1| \leq L_1$, $\left|\frac{\partial f_1}{t}\right| \leq L_2$, $\left|\frac{\partial f_1}{x_1}\right| \leq L_3$, $\left|\frac{\partial f_1}{x_2}\right| \leq L_4$, $\left|\frac{\partial f_1}{z_1}\right| \leq L_5$, $\left|\frac{\partial f_1}{z_2}\right| \leq L_6$, $\left|\frac{\partial f_1}{w_1}\right| \leq L_7$, $\left|\frac{\partial f_1}{u_1}\right| \leq L_8$ and $\left|\frac{\partial f_1}{u_2}\right| \leq L_9$, $|f_2| \leq M_1$, $\left|\frac{\partial f_2}{t}\right| \leq M_2$, $\left|\frac{\partial f_2}{x_1}\right| \leq M_3$, $\left|\frac{\partial f_2}{x_2}\right| \leq M_4$, $\left|\frac{\partial f_2}{z_1}\right| \leq M_5$, $\left|\frac{\partial f_2}{z_2}\right| \leq M_6$, $\left|\frac{\partial f_2}{w_2}\right| \leq M_7$, $\left|\frac{\partial f_2}{u_1}\right| \leq M_8$ and $\left|\frac{\partial f_2}{u_2}\right| \leq M_9$, for any $\|\boldsymbol{u}\|_\infty \leq \Delta_u$, $\|\dot{\boldsymbol{u}}\|_\infty \leq \Delta_{du}$, $|\boldsymbol{s}| \leq \Delta_s$, $\|\boldsymbol{w}\|_\infty \leq \Delta_w$ and $\|\dot{\boldsymbol{w}}\|_\infty \leq \Delta_{dw}$.

Assumption 4 indicates that, there exists a positive constant $L > 0$ and $M > 0$ such that nonlinear mapping $f_{o,1}(\cdot, \cdot, \cdot, \cdot, \cdot, \cdot, \cdot, \cdot)$ is uniformly bounded by this constant L and $f_{o,2}(\cdot, \cdot, \cdot, \cdot, \cdot, \cdot, \cdot, \cdot)$ is uniformly bounded by this constant M provided that Assumptions 1, 2, 3 and 4 hold.

Firstly, Σ_1 (29) is considered, a third-order ESO ($\hat{\Sigma}_1$) thus is designed to estimate the state, uncertainties and disturbances. A new ESO is proposed for the system (29).

$$\begin{aligned} \dot{\hat{x}}_1 &= \hat{x}_2 + C_1\tilde{x}_1 \\ \dot{\hat{x}}_2 &= \hat{x}_3 + \tilde{x}_1 + C_2\tilde{x}_2 + bu_1 + G_0 \\ \dot{\hat{x}}_3 &= \tilde{x}_2 + C_3\tilde{x}_3 \end{aligned} \tag{38}$$

where $C_i > 0, i = 1, 2, 3$ are the design parameters. The control input is coming from (37). From (29) and (38), the estimation error dynamics can be written as

$$\begin{aligned} \dot{\tilde{x}}_1 &= \tilde{x}_2 - C_1\tilde{x}_1 \\ \dot{\tilde{x}}_2 &= \tilde{x}_3 - \tilde{x}_1 - C_2\tilde{x}_2 \\ \dot{\tilde{x}}_3 &= f_{o,1}(t, x_1, x_2, z_1, z_2, w_1, \tilde{u}_1, \tilde{u}_2) - \tilde{x}_2 - C_3\tilde{x}_3 \end{aligned} \tag{39}$$

where $f_{o,1}(t, x_1, x_2, z_1, z_2, w_1, \tilde{u}_1, \tilde{u}_2)$ is defined in (31) and $|\hat{\boldsymbol{x}}(0)| \leq \Delta_s$, where Δ_s is some constant such that this constant can be satisfied. From (39), we can compute

$$\begin{aligned} \tilde{x}_2 &= \dot{\tilde{x}}_1 + C_1\tilde{x}_1 \\ \tilde{x}_3 &= \dot{\tilde{x}}_2 + \tilde{x}_1 + C_2\tilde{x}_2 \end{aligned} \tag{40}$$

The block diagram of ESO is shown in Fig. 5.

Remark 5: Different from the existing ESO in literature [14]–[17], instead of using only measurable $\tilde{x}_1$, the estimation error of $\widetilde{x}_2$ and $\widetilde{x}_3$ are calculated to provide feedback in the design of ESO. ◦

Remark 6: It is noted that in practice, calculating numerically of these two signals from $\widetilde{x}_1$ might be problematic due to existence of measurement noises. Appropriate low-pass filters are thus needed in implementation at the cost of the existence of steady-state error. In the analysis, it is assumed that $\dot{\widetilde{x}}_2$ and $\dot{\widetilde{x}}_3$ can be calculated with enough accuracy. ◦

C. MODEL-GUIDED DATA-DRIVEN CONTROL DESIGN

With the help of ESO, a data-driven control can be designed for the system Σ_1 (29) to cancel the influence of disturbances. The closed loop system with the controller coming from (36) to (37) becomes

$$\begin{aligned}\dot{e}_1 &= x_2\\ \dot{x}_2 &= G_0 + x_3 + b\left(u_{1,md} + (u_1 - u_{1,md})\right)\\ &= x_3 - k_1 e_1 - k_2\hat{x}_2 - \hat{x}_3 + b(u_1 - u_{1,md}).\end{aligned} \tag{41}$$

After the computation, the dynamics of the x_2 can be re-written as

$$\dot{x}_2 = -k_1 e_1 - k_2 x_2 + k_2\tilde{x}_2 + \tilde{x}_3 + b(u_1 - u_{1,md}). \tag{42}$$

Let $\boldsymbol{e} = \begin{bmatrix} e_1 \\ x_2 \end{bmatrix}$. Consequently, it has

$$\dot{\boldsymbol{e}} = \begin{bmatrix} 0 & 1 \\ -k_1 & -k_2 \end{bmatrix}\boldsymbol{e} + \begin{bmatrix} 0 \\ \tilde{x}_3 + k_2\tilde{x}_2 + b(u_1 - u_{1,md}) \end{bmatrix}. \tag{43}$$

Let $A_s = \begin{bmatrix} 0 & 1 \\ -k_1 & -k_2 \end{bmatrix}$ and $B_s = \begin{bmatrix} 0 \\ 1 \end{bmatrix}$. With the consideration of ESO, the closed loop system (43) can be re-written as

$$\begin{aligned}\dot{\boldsymbol{e}} &= A_s\boldsymbol{e} + B_s\left(\tilde{x}_3 + k_2\tilde{x}_2 + b(u_1 - u_{1,md})\right)\\ \dot{\tilde{x}}_1 &= \tilde{x}_2 - C_1\tilde{x}_1\\ \dot{\tilde{x}}_2 &= \tilde{x}_3 - \tilde{x}_1 - C_2\tilde{x}_2\\ \dot{\tilde{x}}_3 &= f_o(t, x_1, x_2, z_1, z_2, w_1, u_1, u_2) - \tilde{x}_2 - C_3\tilde{x}_3\end{aligned} \tag{44}$$

The stability of the system (44) is presented in the following theorem.

Theorem 1: Assume that Assumptions 1, 2, 3 and 4 hold. It is assumed that the parameters k_1 and k_2 are selected satisfying Remark 2. For any given positive parameter set $(\Delta_u, \Delta_{du}, \Delta_s, \Delta_w, \Delta_{dw}, \nu)$ and any positive parameter C_1, there exist $\beta_e \in \mathcal{KL}$, positive constants $\tau_{1,a}, \tau_{1,b}, C_2^* > 0$ and $C_3^* > 0$ such that for any $C_2 \geq C_2^*, C_3 \geq C_3^*, \tau_1 \in [\tau_{1,a}, \tau_{1,b}]$ the following inequalities holds

$$\left\|\begin{bmatrix}\boldsymbol{e}(t)\\ \widetilde{x}(t)\end{bmatrix}\right\| \leq \beta_e\left(\left\|\begin{bmatrix}\boldsymbol{e}(0)\\ \widetilde{x}(0)\end{bmatrix}\right\|, t\right) + \nu \tag{45}$$

for any $\left\|\begin{bmatrix}\boldsymbol{e}(0)\\ \widetilde{x}(0)\end{bmatrix}\right\| \leq 2\Delta_s$.

Proof: Let a Lyapunov candidate be $W(\boldsymbol{e}, \widetilde{\boldsymbol{x}}) = V_1(\boldsymbol{e}) + V(\widetilde{\boldsymbol{x}}) = \boldsymbol{e}^T P\boldsymbol{e} + \frac{1}{2}\tilde{x}_1^2 + \frac{1}{2}\tilde{x}_2^2 + \frac{1}{2}\tilde{x}_3^2$.

For any $\nu \leq \left\|\begin{bmatrix}\boldsymbol{e}\\ \widetilde{x}\end{bmatrix}\right\| \leq 2\Delta_s$. For the given ν, there exists $\epsilon_0 \leq \frac{\nu\lambda_{min}(Q)}{8|b||P||B_s|}$ such that $-\frac{\lambda_{min}(Q)}{4}\boldsymbol{e}^T\boldsymbol{e} + 2\,|\boldsymbol{e}|\,|P|\,|B_s|\,|b|\,\epsilon_0 \leq 0$. Here $\lambda_{min}(Q)$ is the smallest positive eigenvalue of symmetric positive definite matrix Q. Then for this given ϵ_0, using Remark 4, the bound for $\tau_{1,a}$ and $\tau_{1,b}$ can be obtained accordingly.

The derivative of $W(\cdot,\cdot)$ along the trajectories of (44) becomes

$$\begin{aligned}\dot{W}(\boldsymbol{e}, \widetilde{x}) &= \boldsymbol{e}^T(A_s^T P + PA_s)\boldsymbol{e}\\ &\quad + (\boldsymbol{e}^T PB_s + B_s^T P\boldsymbol{e})\left(\tilde{x}_3 + k_2\tilde{x}_2 + b(u_1 - u_{1,md})\right)\\ &\quad + \tilde{x}_1\cdot\tilde{x}_2 - C_1\cdot\tilde{x}_1^2 + \tilde{x}_2\cdot\tilde{x}_3 - \tilde{x}_2\cdot\tilde{x}_1 - C_2\cdot\tilde{x}_2^2\\ &\quad + \tilde{x}_3 f_{o1} - \tilde{x}_2\cdot\tilde{x}_3 - C_3\cdot\tilde{x}_3^2\\ &\leq -\boldsymbol{e}^T Q\boldsymbol{e} + 2|\boldsymbol{e}||P||B_s|\,(|\tilde{x}_3| + k_2|\tilde{x}_2| + b|\epsilon_0|)\\ &\quad - C_1\tilde{x}_1^2 - C_2\tilde{x}_2^2 - \frac{C_3}{2}\tilde{x}_3^2 - \left(\frac{C_3}{2}\tilde{x}_3^2 - L\cdot|\tilde{x}_3|\right).\\ &\leq -\frac{\lambda_{min}(Q)}{4}|\boldsymbol{e}|^2 - C_1\tilde{x}_1^2\\ &\quad - \left(\frac{\sqrt{\lambda_{min}(Q)}}{2}|\boldsymbol{e}| - \frac{2}{\sqrt{\lambda_{min}(Q)}}|P||B_s||k_2||\tilde{x}_2|\right)^2\\ &\quad - \left(\frac{\sqrt{\lambda_{min}(Q)}}{2}|\boldsymbol{e}| - \frac{2}{\sqrt{\lambda_{min}(Q)}}|P||B_s||\tilde{x}_3|\right)^2\\ &\quad - \left(\frac{C_3}{2}\tilde{x}_3^2 - L\cdot|\tilde{x}_3|\right).\end{aligned} \tag{46}$$

For any L there exists $C_2^* = \frac{4(|P||B_s||k_2|)^2}{\lambda_{min}(Q)}$ and $C_3^* = \max\left\{\frac{4(|P||B_s|)^2}{\lambda_{min}(Q)}, \frac{2L}{\nu}\right\}$ such that for any $C_2 > C_2^*$ and $C_3 > C_3^*$, $\left(\frac{C_3}{2}\tilde{x}_3^2 - L\cdot|\tilde{x}_3|\right) \geq 0$.

Consequently, it leads to

$$\begin{aligned}\dot{W}(\boldsymbol{e}, \widetilde{x}) \leq &-\frac{\lambda_{min}(Q)}{4}|\boldsymbol{e}|^2 - C_1\tilde{x}_1^2\\ &- \left(\frac{\sqrt{\lambda_{min}(Q)}}{2}|\boldsymbol{e}| - \frac{2}{\sqrt{\lambda_{min}(Q)}}|P||B_s||k_2||\tilde{x}_2|\right)^2\\ &- \left(\frac{\sqrt{\lambda_{min}(Q)}}{2}|\boldsymbol{e}| - \frac{2}{\sqrt{\lambda_{min}(Q)}}|P||B_s\|\tilde{x}_3|\right)^2\end{aligned} \tag{47}$$

for any $\nu \leq \left\|\begin{bmatrix}\boldsymbol{e}\\ \widetilde{x}\end{bmatrix}\right\| \leq 2\Delta_s$. This completes the proof. ◦

Remark 7: Theorem 1 shows that by combining medel-guided state feedback control with data-driven control designed on the basis of ESO, the closed loop system is well-behaved, that is, by tuning the parameters, the ultimate bound ν can be made arbitrarily small. ◦

Similar to Σ_1, the same control method can be designed for Σ_2 (30), then the control objective can be achieved, the output $\boldsymbol{y}$ will be able to track the desired set-point (r_1, r_2) and the effects of the uncertainties, disturbances and coupling will be reduced. The block diagram of model-guided data-driven control for a half bogie of the maglev system is shown in Fig. 6.

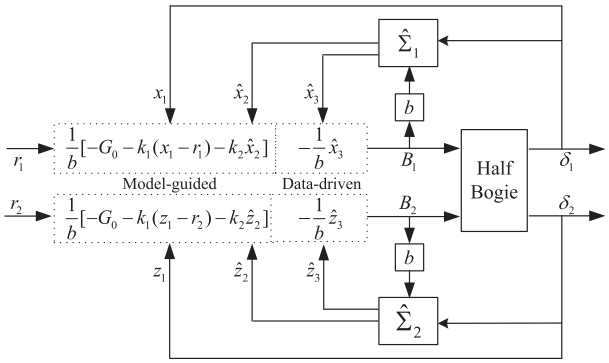

FIGURE 6. Block diagram of model-guided data-driven control for a half bogie of the maglev system.

The design principle of this model-guided data-driven method is different from the traditional model-free ADRC with ESO. The design procedure of the proposed method is:

(1) Design a stabilizing state-feedback controller for a nominal model.
(2) Design an ESO using on-line measurements to estimate the needed state and lumped uncertainties
(3) Design an ADRC to only cancel the influence of lumpled uncertainties.

This procedure is different from the traditional ADRC with ESO, which has the following design procedure:

(1) Design an ESO to estimate unknown state and lumped uncertainties
(2) Design an ADRC to cancel the effect of lumped uncertainties and provide a full-state feedback to stabilize the system using the estimated states.

In this traditional design, the ideal case is to design ESO and ADRC separately. In general, this separation design is hard. It is possible if the gain of ESO is sufficiently large so that the response of ESO is much faster than that of ADRC. Moreover, this separation design also requires that the ESO can work. In the literature of ESO [12], [13], [22], it is always required that in order to ensure that the ESO can work, the response of the system with some input signals needs to be uniformly bounded. In general, designing an ESO requires that the system is open loop stable.

On the other hand, in the proposed model-guided data-driven method, the model plays an important role to design the stabilizing controller and ensure the boundedness of trajectories. The role of ADRC is only to cancel the lumped uncertainties while ESO is to used to estimate the lumped uncertainties and the needed state. As the ESO only estimate unknown part, it is not a surprise that a low gain ESO can work. It is noted that even though the stabilizing controller and the ARDC with ESO are designed separately, none of them needs a high gain to separate the time-scale. Both ESO and the stabilizing controller can work slowly as observed in some applications.

This design philosophy is widely used for engineering practitioners. It is usually hard to directly used data-driven method without knowing anything about the system.

IV. SIMULATIONS AND EXPERIMENTAL RESULTS

In order to evaluate the performance of the proposed model-guided data-driven control law, it is tested using simulations and a small scale half bogie experimental platform, as shown in Fig. 7.

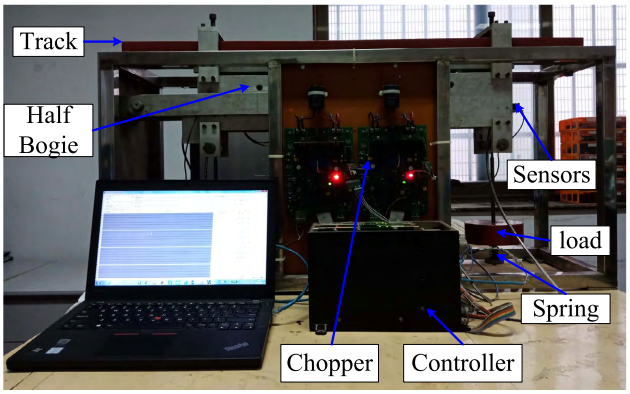

FIGURE 7. Small scale half bogie experiment platform.

The half bogie consists of SP1 and SP2. The control objective is to levitate SP1 and SP2 to the desired set-point.

This platform can be modeled by (19) with parameters identified using experimental results and standard system identification techniques such as least square estimation. The values of parameters are summarized in Table 1.

TABLE 1. Parameters identified for the small scale half bogie experiment platform.

Parameters	Description	Value
μ_0	permeability of vacuum	$4\pi \times 10^{-7} N \cdot A^{-2}$
g	accelerate of gravity	$9.81m \cdot s^{-2}$
A	effective area of per electromagnet	$0.0014m^2$
N	coil turns Number of per electromagnet	540
R	Coil resistance of per electromagnet	2.1Ω
l	length of a bogie	$0.65m$
m	mass of a bogie	$5.2kg$
M	mass of load	$16kg$

With the consideration of physical and hardware limitations, some variables are constrained in some closed set. That is, $\delta \in [1mm, 10.5mm]$, $\dot{\delta} \in [-50m/s, 50m/s]$, $\ddot{\delta} \in [-50m/s^2, 50m/s^2]$ and $B \in [0T, 0.7T]$.

In order to test the effectiveness of the proposed model-guided data-driven method, both simulations and experiments are arranged. The role of simulations is to show performance of the proposed method with respect to different tuning parameters in order to provide insights for engineers. The robustness of the proposed model-guided data-driven controller is tested when different loads are added to the system.

Moreover, two comparisons will be performed. The first one is the proposed model-guided data-driven method is compared with model-guided control design using the nominal model. The second compares the proposed model-guided data-driven method with the standard ADRC with ESO.

Consistent with the experimental platform, the simulation model consists of the model (19), chopper and filtering blocks. Each subsystem is approximated by a lower order linear system with parameters identified from well-designed experiments. Measurement noises are considered in simulations as white noises (zero mean and variance is $0.01mm$). Same as the experimental platform, the sampling frequency of the system and the controller is set to $4000Hz$. The initial gap of the two suspension points is set to $10.5mm$ and the set point is selected as $r = 6mm$. In order to check the robustness of the proposed model-guided data-driven algorithm, after the suspension points are stabilized at the set point, the SP1 is set to track a square wave signal with period 1 mm. Appropriate saturation functions are used in order to take the physical constraints of the platform into consideration.

A. SIMULATION RESULTS

1) DESIGN PROCEDURE

The design procedure in simulation is consistent with that stated in Theorem 1, as summarized as follows:

(1) Design the model-guided state feedback controller based on the nominal model. As the input is already bounded from the physical constraints. The feedback gains k_1 and k_2 need to satisfy Remark 2 and Assumptions 1.

(2) Design the ESO from measurements with the ADRC to estimate system state and lumped uncertainties on-line. Tuning parameters are: (C_1, C_2, C_3, τ_1).
Usually, C_1, C_2 and C_3 should be large enough to ensure that the estimated state converges sufficiently fast to the a smaller neighborhood of the true state (or ultimate bound ν in Theorem 1). Due to existence of measurement noises, larger values of (C_1, C_2, C_3) would amplify noises. This can degrade the tracking performance and even lead to unstable performance. There is a design trade-off.
The parameter τ_1 in filtering is designed on the basis of Theorem 1. The tuning guideline was highlighted in Remark 4 to satisfy Assumptions 1 and Assumptions 2.

(3) Re-tuning parameters based on the closed loop performance and control effort. This procedure will be repeated until good performance is obtained.

2) MODEL-GUIDED CONTROL DESIGN

Based on the nominal model, firstly, a state feedback control is designed. By trial and error method, using the complex simulation model (including (19) and other blocks appeared in experimental setup, the parameters in simulations are set as $k_1 = 4500$, $k_2 = 500$ to achieve a reasonably good tracking performance.

In order to test the robustness of the controller, SP1 is required to track a square wave while SP2 will track the desired set-point. The simulation results are shown in Fig. 8.

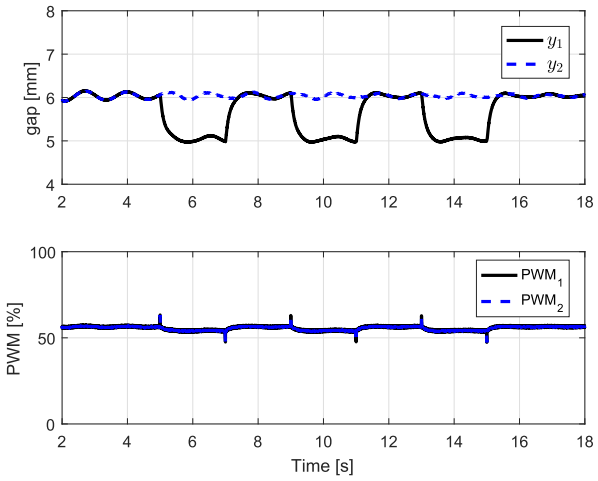

FIGURE 8. Tracking performance using model-guided feedback control (simulation).

It is observed, as the model-guided feedback control law is based on the nominal model, which is much simper than the simulated model, the boundedness of the trajectories is guaranteed. The tracking performance is reasonable, though oscillations and steady-state errors exist. This results have demonstrate the limitation of model-guided control design. Some data-driven techniques are needed to enhance the robustness with respect to disturbances and uncertainties.

This model-guided control law with the same tuning parameters are used in our model-guided data-driven control design with ESO.

3) MODEL-GUIDED DATA-DRIVEN CONTROL WITH ESO

After designing the state feedback control, the ESO is designed with the proposed model-guided data-driven controller u_1. The parameters are selected as $(C_1, C_2, C_3, \tau_1) = (300, 300, 300, 600)$ which obviously satisfy conditions needed in Theorem 1. The simulation results is shown in Fig. 9.

It can be shown that when the data-driven controller is combined with the model-guided controller, the performance of the closed loop system has been improved.

Next, it will discuss the effects of tuning parameters on the performance of the proposed control algorithm.

a: EFFECT OF (C_1, C_2, C_3)

Let the model-guided feedback gain is fixed as before and $\tau = 300$ be fixed. In order to test the effects of these three tuning parameters, three sets of parameters are selected.

a $C_1 = C_2 = C_3 = 500$
b $C_1 = C_2 = C_3 = 300$
c $C_1 = C_2 = C_3 = 100$

The simulation results in terms of tracking are shown in Fig. 10 for two suspension points. The performance of

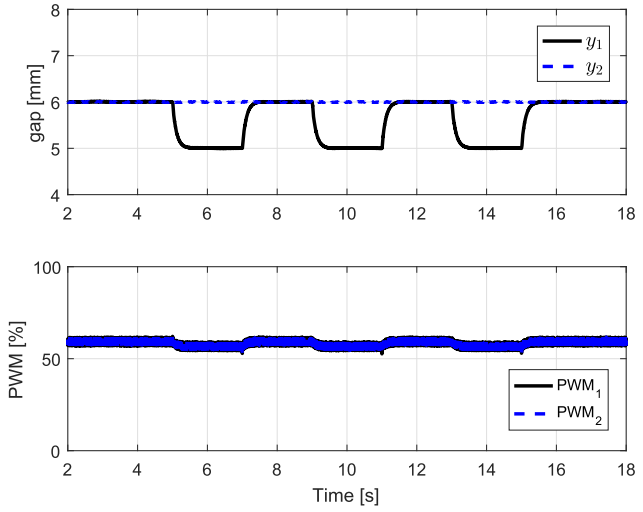

FIGURE 9. Tracking performance using the proposed control (simulation).

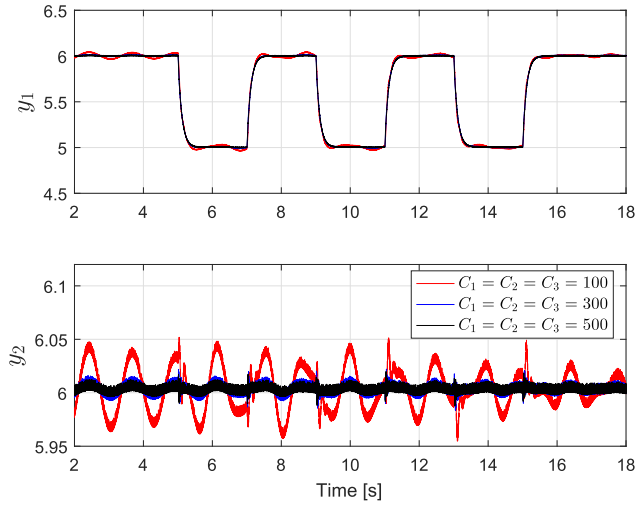

FIGURE 10. Tracking performance using the proposed control law with different (C_1, C_2, C_3) (simulation).

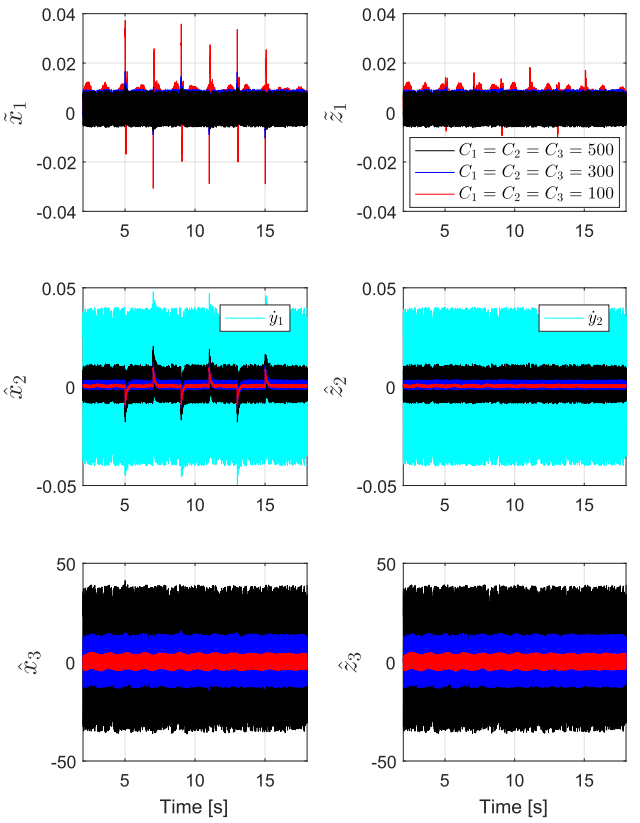

FIGURE 11. Estimation performance using the proposed control law with different (C_1, C_2, C_3) (simulation).

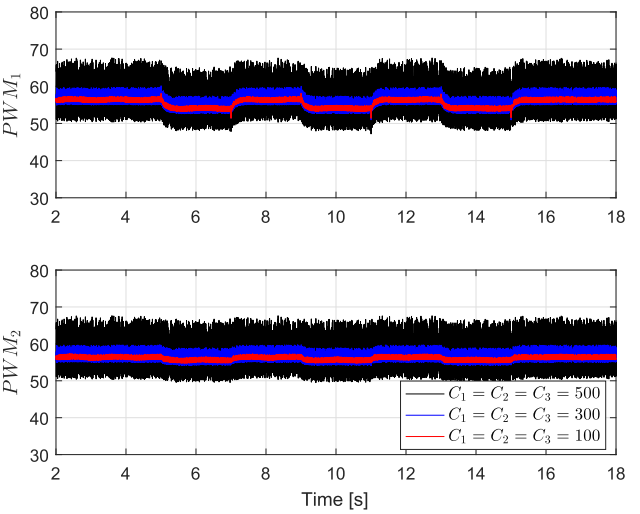

FIGURE 12. Control effort using the proposed control law with different (C_1, C_2, C_3) (simulation).

ESO in terms of estimation errors of SP1 and SP2 is shown in Fig. 11. The control input in terms of PWM signals for SP1 and SP2 are presented in Fig. 12.

It is observed that large values of (C_1, C_2, C_3) will lead to faster convergence speed of the estimated state to the actual state. However, due to the existence of white noises, larger values of (C_1, C_2, C_3) will introduce large variations of control input, leading to larger PWM signals and requiring more energy consumption from actuators.

b: EFFECT OF τ_1

The role of the tuning parameter of τ_1 is to ensure that the control input signal cannot change too fast. When τ_1 tends to ∞, there is no filtering for the control input signal, leading to a smaller ultimate bound (ν in Theorem 1). A smaller τ_1 indicates that the high frequency component of the control input is attenuated, leading to a relatively more smooth control input. This filter also can reject high-frequency noises. However, as some information of control input is attenuated, this might lead to a larger ultimate bound. There is another design trade-off.

In order to test the effects of τ_1, three sets of τ_1 are selected with other tuning parameters are fixed as

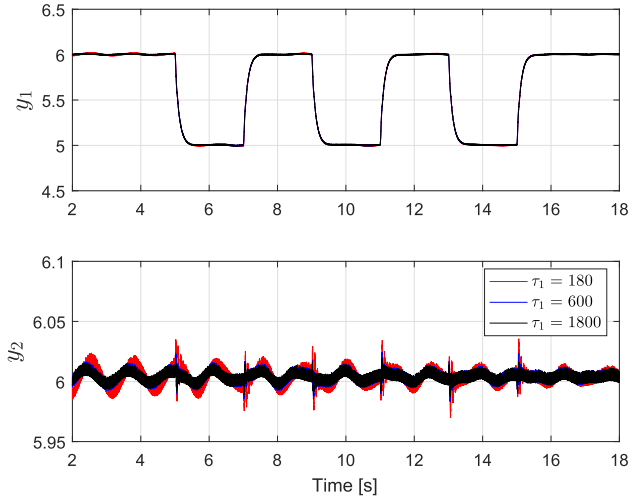

FIGURE 13. Tracking performance using the proposed control law with different τ_1 (simulation).

$(C_1, C_2, C_3) = (300, 300, 300)$ and the model-guided control law is also fixed as before.

a $\tau_1 = 1800$
b $\tau_1 = 600$
c $\tau_1 = 180$

The simulation results in terms of tracking are shown in Fig. 13 for two suspension points. The performance of ESO in terms of estimation errors of SP1 and SP2 is shown in Fig. 14 The control input in terms of PWM signals for SP1 and SP2 are presented in Fig. 15

It can be seen that the selection of τ_1 in filter does not affect the estimation performance ESO, but it affects the tracking performance and the control input signal. A smaller parameter τ_1 will lead to larger tracking error. But the variation of control input signal is smaller.

c: ROBUSTNESS WITH RESPECT TO DIFFERENT LOADS

In order to show the robustness of the proposed method, different loads are added to the half-bogie. Three sets of the loads M are selected.

a $M = 16kg$
b $M = 22kg$
c $M = 31kg$

The parameters are selected as $(k_1, k_2, C_1, C_2, C_3, \tau_1) = (4500, 500, 300, 300, 300, 600)$. Simulation results in terms of tracking are shown in Fig. 16 for two suspension points. The performance of ESO in terms of estimation errors of SP1 and SP2 is shown in Fig. 17 The control input in terms of PWM signals for SP1 and SP2 are presented in Fig. 18.

This shows that the proposed model-guided data-driven control algorithm is quite robust to different loads. It can be seen that the tracking performance, estimation performance of ESO and not sensitive to the load change. As the load increases, it leads to a larger lumped uncertainty.

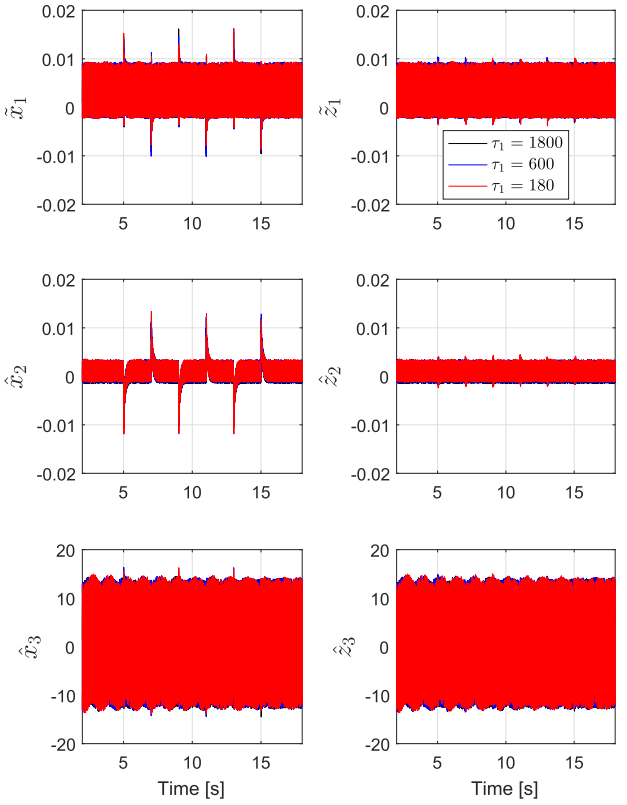

FIGURE 14. Estimation performance using the proposed control law with different τ_1 (simulation).

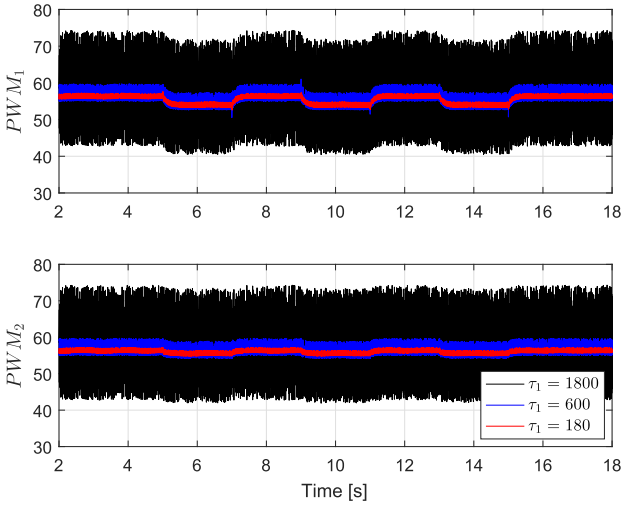

FIGURE 15. Control effort using the proposed control law with different τ_1 (simulation).

Consequently $\hat{x}_3$ and $\hat{z}_3$ have to increase, resulting in larger control input signals PWM_1 and PWM_2.

4) MODEL-FREE ADRC WITH ESO

As pointed out early, the proposed model-guided data-driven method is quite different from the traditional ADRC method with ESO. The parameters of the proposed method are fixed as in the previous subsection.

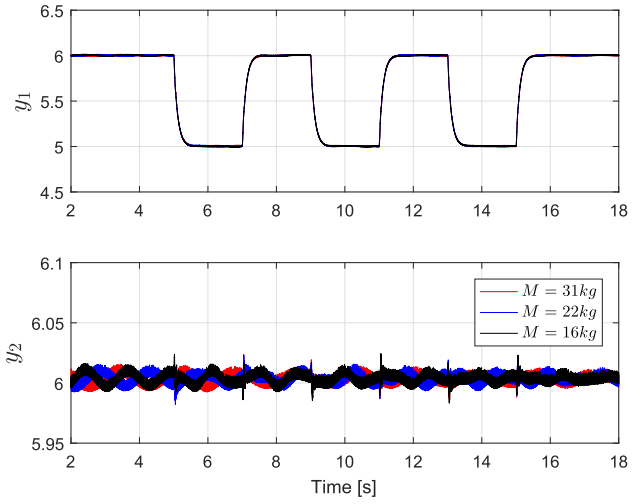

FIGURE 16. Tracking performance using the proposed control law with different loads (simulation).

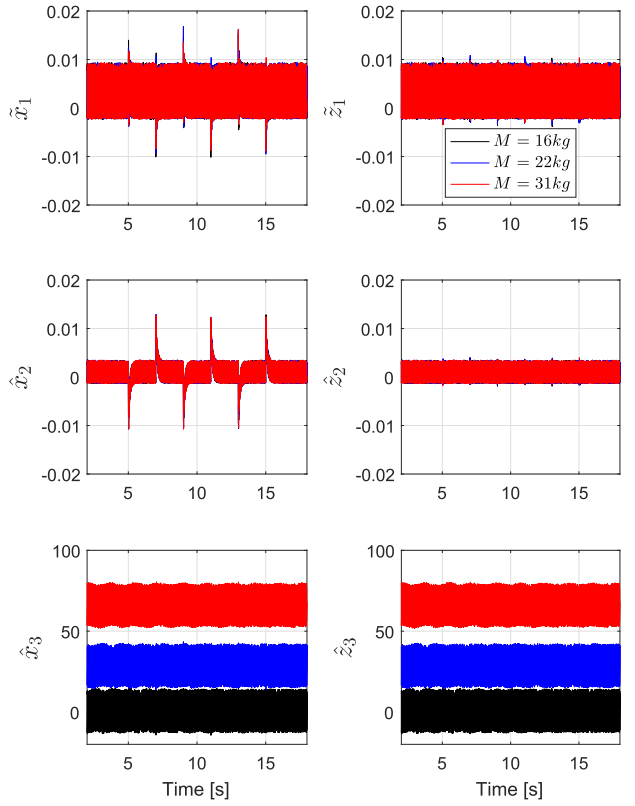

FIGURE 17. Estimation performance using the proposed control law with different loads (simulation).

As the Maglev system is an open loop unstable system, designing an ESO directly is quite challenging. It is noted that when all physical constraints are removed in simulations, the model-free ADRC with ESO cannot work as ESO cannot ensure the convergence of estimation error when the system is an open loop unstable.

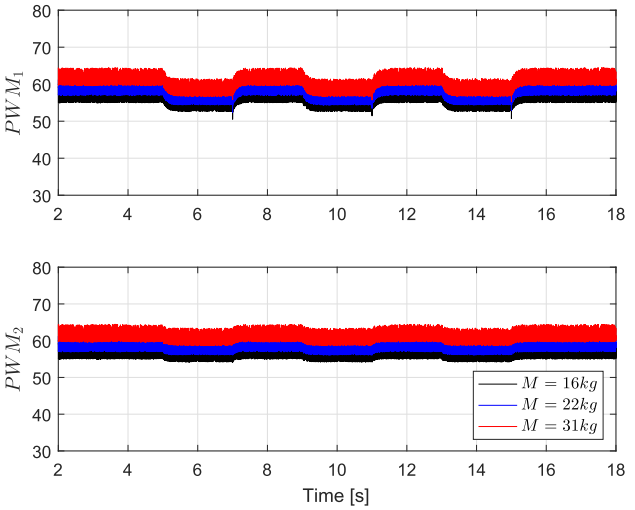

FIGURE 18. Control effort using the proposed control law with different loads (simulation).

With the consideration of the physical constraints from the system and appropriate saturation functions, the boundedness of trajectories can be ensured. With the fixed initial condition, by trying different values of (C_1, C_2, C_3), it is observed that when (C_1, C_2, C_3) are smaller than $(100, 210, 220)$ and τ_1 is smaller than 360, the estimation error of the ESO is divergent. If ESO is not working, the model-free ADRC cannot work either. However, the proposed model-guided data-driven method can less sensitive to the choice of (C_1, C_2, C_3).

In the case when both methods are working, the same tuning parameters set is used to do a fair comparison. The tracking performance of the proposed model-guided data-driven method and the model-free ADRC with ESO is shown in Fig. 19. The performance of ESO in terms of estimation errors of SP1 and SP2 is shown in Fig. 20 The control input in terms of PWM signals for SP1 and SP2 are presented in Fig. 21

It can be seen that two methods with the same tuning parameters have similar tracking performance. The estimation performance of ESO for two state signals $(\hat{x}_1(\hat{z}_1), \hat{x}_2(\hat{z}_2)$ is quite similar. Obviously, as two designs estimate different lumped uncertainties $\hat{x}_3(\hat{z}_3)$. The ESO in the model-free setting estimates larger lumped uncertainties, which include the nominal model as can be seen in Fig. 20. Consequently, the control input of the proposed model-guided data-driven method is smaller than the model-free method as shown in Fig. 21. This feature is quite attractive as reducing energy consumption of actuators is always preferred.

B. EXPERIMENT RESULTS

Similar to simulation results, a few different experiments were arranged to test the performance of model-guided control law, the proposed model-guided data-driven method, and model-free method.

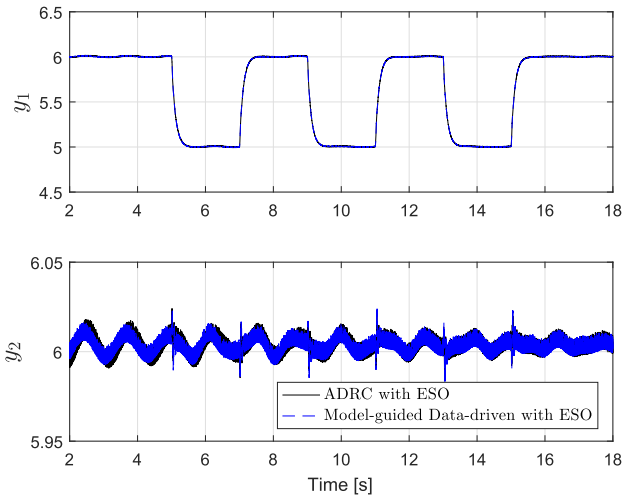

FIGURE 19. Tracking performance: comparing the proposed control law with the model-free method (simulation).

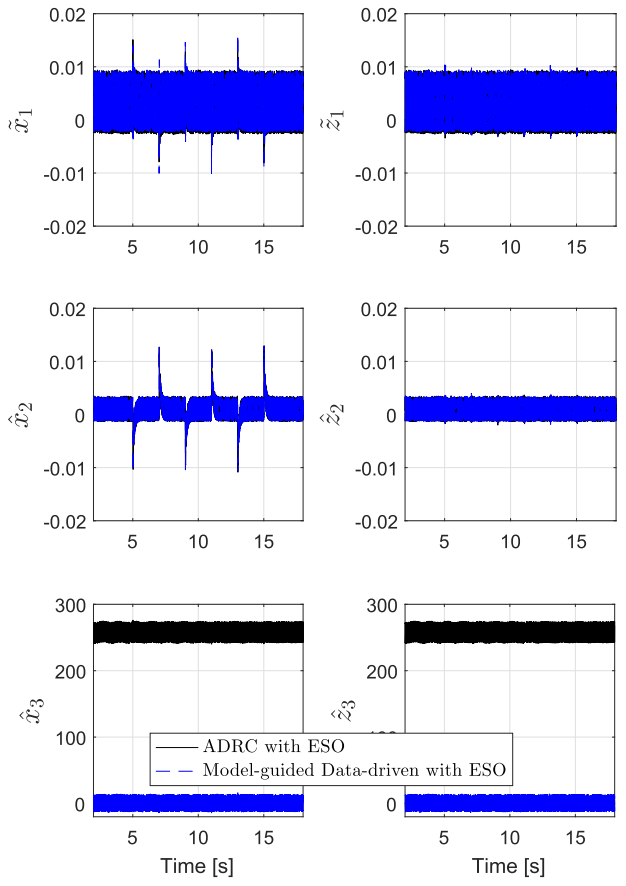

FIGURE 20. Estimation performance: comparing the proposed control law with the model-free method (simulation).

1) MODEL-GUIDED CONTROL DESIGN

Based on the known information of the half bogie model and a large number of experiments, a reasonable set parameters has been obtained which can achieve a reasonable tracking

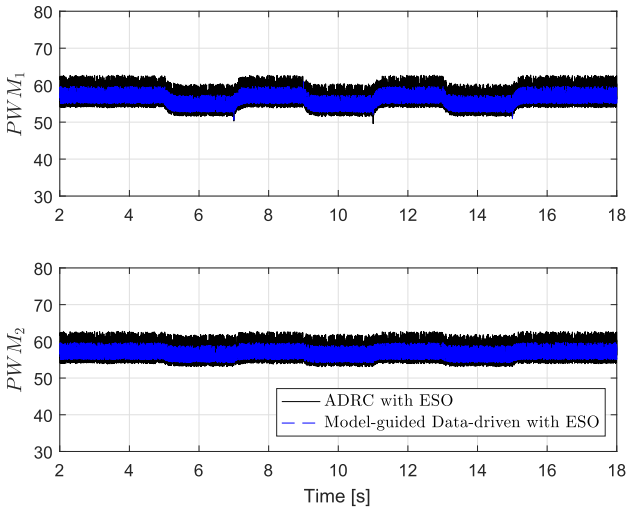

FIGURE 21. Control effort: comparing the proposed control law with the model-free method (simulation).

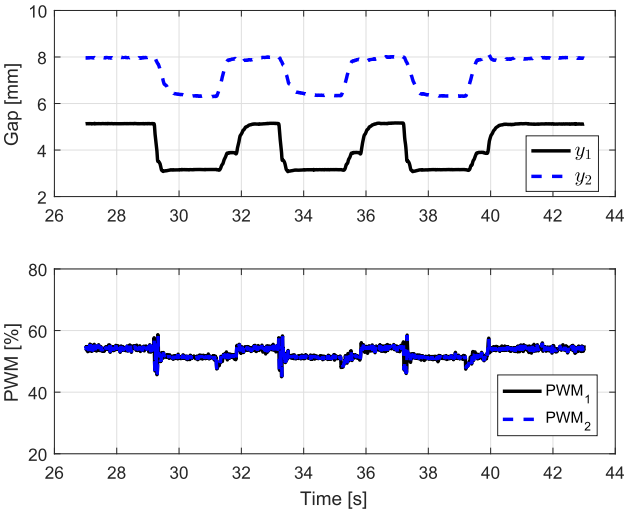

FIGURE 22. Tracking performance using model-guided controller (experiment).

performance. Parameters for experiments are selected as $k_1 = 3900$, $k_2 = 400$, which is slightly conservative than the simulations to avoid possible unacceptable overshoots in the tracking.

Experimental results are shown in Fig. 22. From experiment results, it can be seen that the model based controller can ensure the boundedness of trajectories, But the tracking performance is not good with obvious steady-state errors. The coupling effect between two suspension points is also apparent as the tracking performance of SP1 is quite different from that of SP2.

When comparing the simulation results and experiment results, it is not hard to conclude that the simulation model, which is identified from experiments, is still not sufficiently accurate.

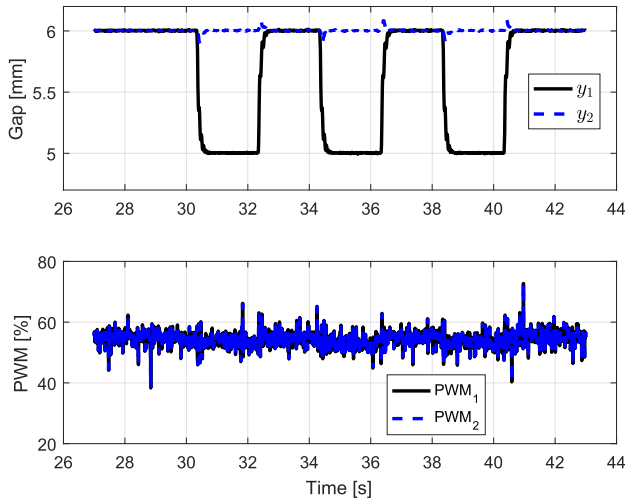

FIGURE 23. Tracking performance and control effort using the proposed controller (experiment).

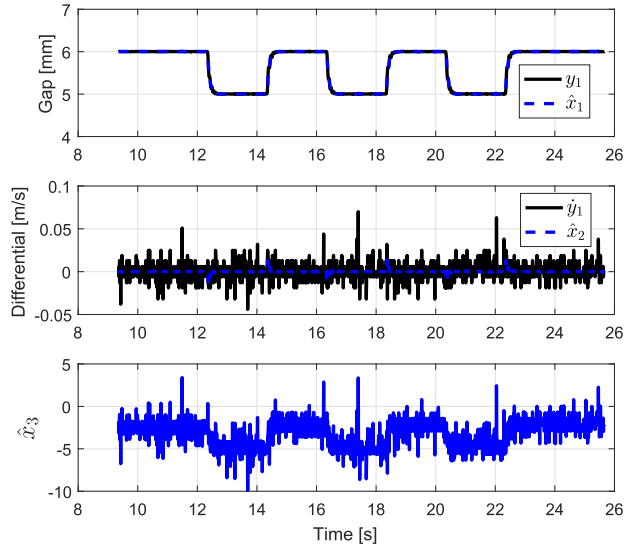

FIGURE 24. Estimation performance of SP1, the proposed method (experiment).

2) MODEL-GUIDED DATA-DRIVEN CONTROL WITH ESO

Similar to simulations results, by a large number of experiments, a set of parameters is selected as $(k_1, k_2, C_1, C_2, C_3, \tau_1) = (3900, 400, 100, 100, 100, 1000)$, in which the feedback gain is obtained from model-guided design. Experimental results in terms of tracking and control effort are shown in Fig. 23. Fig. 24 and Fig. 25 show the performance of estimation using ESO for SP1 and SP2 respectively. It is noted that traditionally, the gap velocity is estimated using the numerical differentiation of the gap measurements. Compared with the numerical differentiation method, ESO can better estimate the gap velocity.

The robustness of the proposed model-guided data-driven method is verified by adding one load with $6kg$ to SP1. Experimental results of SP1 is shown in Fig. 26, which indicates the robustness of the proposed method.

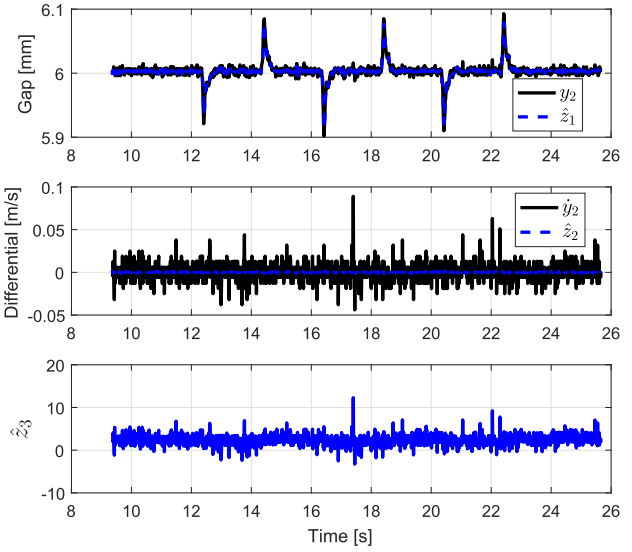

FIGURE 25. Estimation performance of SP2, the proposed method (experiment).

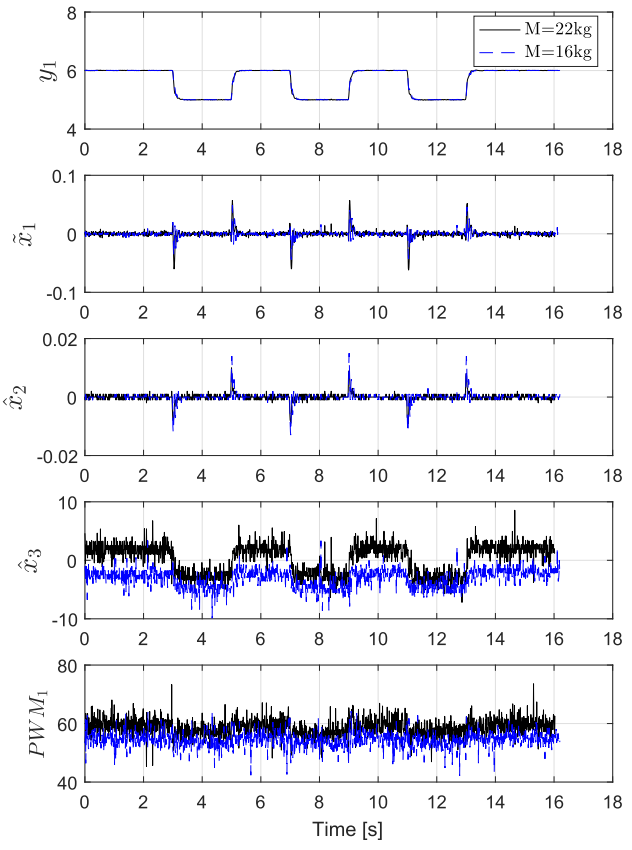

FIGURE 26. Performance of the proposed method with different loads (experiment).

3) MODEL-FREE ADRC METHOD WITH ESO

In order to compare the proposed model-guided data-driven method with a model-free method (ADRC with ESO), the same parameters are selected. Experimental results are shown

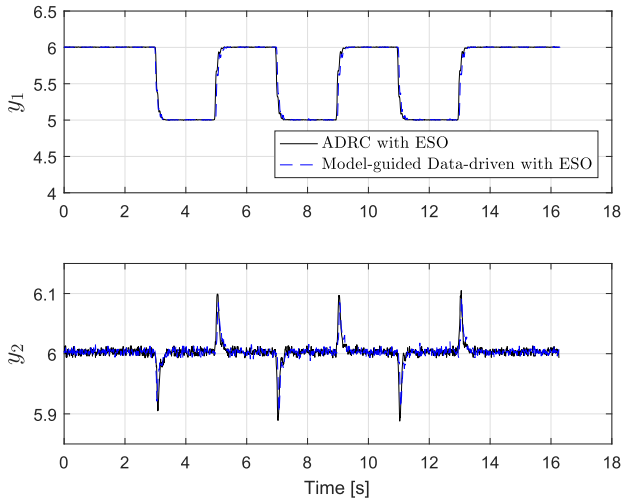

FIGURE 27. Tracking performance: comparing the proposed method with model-free method (experiment).

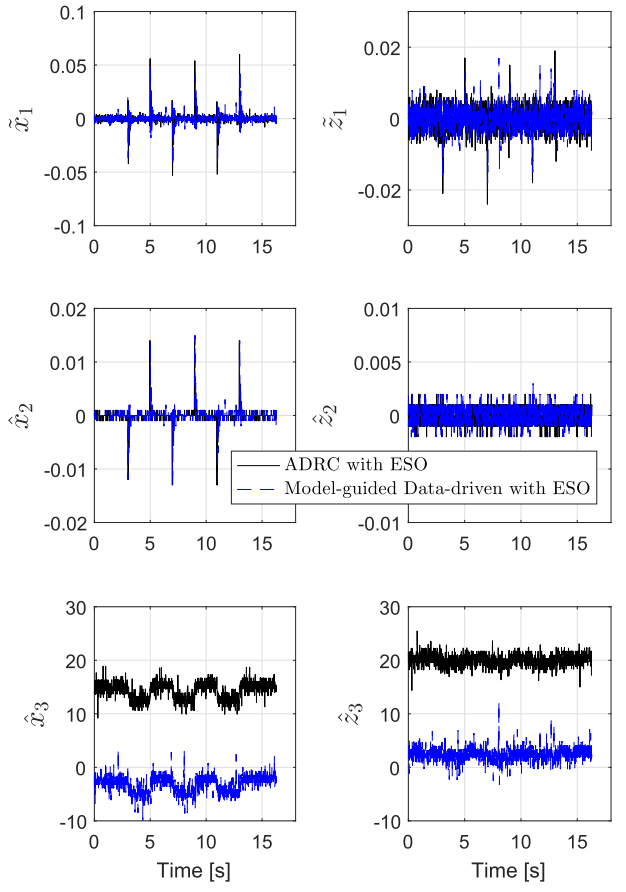

FIGURE 28. Estimation performance: comparing the proposed method with model-free method (experiment).

in Fig. 27, Fig. 28 and Fig. 29. The experimental results are quite similar to simulation results. This again shows that the proposed model-guided data-driven method is quite robust and is able to achieve the good tracking performance with less control effort, when compared with the model-free method.

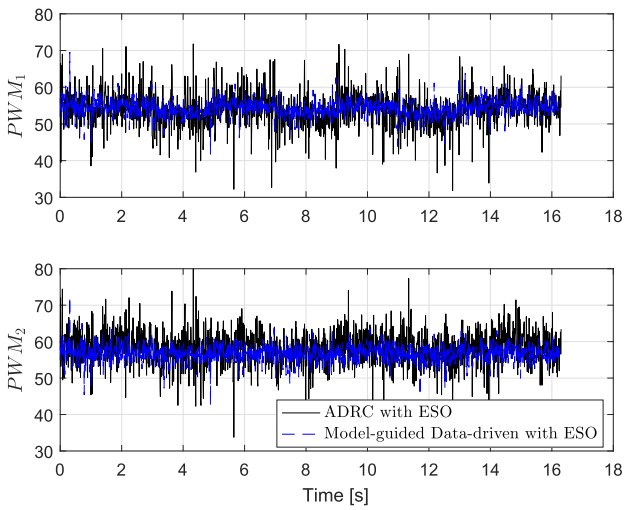

FIGURE 29. Control effort: comparing the proposed method with model-free method (experiment).

V. CONCLUSION

In order to improve the control performance of Maglev systems, a new model-guided data-driven decentralized control has been designed and implemented using both some knowledge of model and measured data. Based on the half bogie model, a state feedback controller was designed to stabilize the system. A new ESO was proposed to estimate unknown system state and un-modelled uncertainties, disturbances and coupling from on-line measurements. Based on this ESO, the effect of un-modeled uncertainties were compensated by the ADRC. By tuning the parameters of state feedback controller and ESO appropriately, the closed loop system can track the desired gap arbitrarily close in the presence of uncertainties, disturbances, and coupling. Simulation and experimental results have validated the effectiveness of the proposed method.

REFERENCES

[1] V. R. Vuchic and J. M. Casello, "An evaluation of maglev technology and its comparison with high speed rail," *Transp. Quart.*, vol. 56, no. 2, pp. 33–49, 2002.
[2] L. Yan, "Development and application of the maglev transportation system," *IEEE Trans. Appl. Supercond.*, vol. 18, no. 2, pp. 92–99, Jun. 2008.
[3] H.-W. Lee, K.-C. Kim, and J. Lee, "Review of maglev train technologies," *IEEE Trans. Magn.*, vol. 42, no. 7, pp. 1917–1925, Jul. 2006.
[4] Y. Luguang, "Progress of the Maglev transportation in China," *IEEE Trans. Appl. Supercond.*, vol. 16, no. 2, pp. 1138–1141, Jun. 2006.
[5] G. R. Chen, L. L. Zheng, and D. F. Zhou, "Study on the characteristics of the maglev electromagnet considering the magnetic field induced by eddy current," *Appl. Mech. Mater.*, vol. 392, pp. 413–419, Sep. 2013.
[6] Y. Liu, W. Deng, and P. Gong, "Dynamics of the bogie of maglev train with distributed magnetic forces," *Shock Vib.*, vol. 2015, Aug. 2015, Art. no. 896410.
[7] Y. Sun, W. Li, D. Chang, and Y. Teng, "Dynamic and decoupling analysis of the bogie with single ems modules for low-speed maglev train," *Adv. Sci. Technol. Lett.*, vol. 121, pp. 83–88, Aug. 2016.
[8] G. He, J. Li, and P. Cui, "Decoupling control design for the module suspension control system in maglev train," *Math. Problems Eng.*, vol. 2015, Dec. 2015, Art. no. 865650.
[9] D. Chen, J. Yin, L. Chen, and H. Xu, "Parallel control and management for high-speed maglev systems," *IEEE Trans. Intell. Transp. Syst.*, vol. 18, no. 2, pp. 431–440, Feb. 2017.

[10] Y. Huang and J. Han, "Analysis and design for the second order nonlinear continuous extended states observer," *Chin. Sci. Bull.*, vol. 45, p. 1938, Nov. 2000.
[11] J. Han, "From PID to active disturbance rejection control," *IEEE Trans. Ind. Electron.*, vol. 56, no. 3, pp. 900–906, Mar. 2009.
[12] B.-Z. Guo and Z.-L. Zhao, "On the convergence of an extended state observer for nonlinear systems with uncertainty," *Syst. Control Lett.*, vol. 60, no. 6, pp. 420–430, 2011.
[13] Z.-L. Zhao and B.-Z. Guo, "A nonlinear extended state observer based on fractional power functions," *Automatica*, vol. 81, pp. 286–296, Jul. 2017.
[14] Y. Huang, H. Wan, and J. Song, "Analysis and design for third order nonlinear continuous extended states observer," in *Proc. 19th Chin. Control Conf.*, 2000, pp. 677–681.
[15] Q. Zheng, L. Q. Gao, and Z. Gao, "On validation of extended state observer through analysis and experimentation," *J. Dyn. Syst., Meas., Control*, vol. 134, no. 2, pp. 024505-1–024505-6, 2012.
[16] Z.-L. Zhao and B.-Z. Guo, "On convergence of the nonlinear active disturbance rejection control for MIMO systems," *SIAM J. Control Optim.*, vol. 51, no. 2, pp. 1727–1757, 2013.
[17] Z.-L. Zhao and B.-Z. Guo, "Extended state observer for uncertain lower triangular nonlinear systems," *Syst. Control Lett.*, vol. 85, pp. 100–108, Nov. 2015.
[18] W. Xue and Y. Huang, "On performance analysis of ADRC for a class of MIMO lower-triangular nonlinear uncertain systems," *ISA Trans.*, vol. 53, no. 4, pp. 955–962, 2014.
[19] Z. Gao, "Active disturbance rejection control: A paradigm shift in feedback control system design," in *Proc. IEEE Amer. Control Conf.*, Jun. 2006, p. 7.
[20] D. Sun, "Comments on active disturbance rejection control," *IEEE Trans. Ind. Electron.*, vol. 54, no. 6, pp. 3428–3429, Dec. 2007.
[21] Q. Zheng, L. Q. Gaol, and Z. Gao, "On stability analysis of active disturbance rejection control for nonlinear time-varying plants with unknown dynamics," in *Proc. 46th IEEE Conf. Decis. Control*, Dec. 2007, pp. 3501–3506.
[22] J. Han, *Active Disturbance Rejection Control Technique-the Technique for Estimating and Compensating the Uncertainties*. Beijing, China: National Defense Industry Press, 2008, pp. 197–270.
[23] Z.-L. Zhao and B.-Z. Guo, "On convergence of nonlinear active disturbance rejection control for SISO nonlinear systems," *J. Dyn. Control Syst.*, vol. 22, no. 2, pp. 385–412, 2016.
[24] Z.-G. Xu, S.-H. Xu, L.-M. Shi, and N.-Q. Jin, "Study on direct fuzzy adaptive control for hybrid magnets used on ems maglev systems," *Proc.-Chin. Soc. Elect. Eng.*, vol. 25, no. 18, p. 157, 2005.
[25] R. J. Wai and J. D. Lee, "Adaptive fuzzy-neural-network control for maglev transportation system," *IEEE Trans. Neural Netw.*, vol. 19, no. 1, pp. 54–70, Jan. 2008.
[26] R.-J. Wai, M.-W. Chen, and J.-X. Yao, "Observer-based adaptive fuzzy-neural-network control for hybrid maglev transportation system," *Neurocomputing*, vol. 175, pp. 10–24, Jan. 2016.
[27] H. Ji, Z. Hou, L. Fan, and F. L. Lewis, "Adaptive iterative learning reliable control for a class of non-linearly parameterised systems with unknown state delays and input saturation," *IET Control Theory Appl.*, vol. 10, no. 17, pp. 2160–2174, Nov. 2016.
[28] J.-H. Li, J. Li, and G. Zhang, "A practical robust nonlinear controller for maglev levitation system," *J. Central South Univ.*, vol. 20, no. 11, pp. 2991–3001, 2013.
[29] D.-S. Liu, J. Li, and W.-S. Chang, "Study on motional coupling of single ems module," *J. China Railway Soc.*, vol. 28, no. 3, pp. 22–26, 2006.
[30] G. He, J. Li, and P. Cui, "Nonlinear control scheme for the levitation module of maglev train," *J. Dyn. Syst., Meas., Control*, vol. 138, no. 7, p. 074503, 2016.
[31] N. F. Al-Muthairi and M. Zribi, "Sliding mode control of a magnetic levitation system," *Math. Problems Eng.*, vol. 2004, no. 2, pp. 93–107, 2004.
[32] J. Yang, S. Li, and X. Yu, "Sliding-mode control for systems with mismatched uncertainties via a disturbance observer," *IEEE Trans. Ind. Electron.*, vol. 60, no. 1, pp. 160–169, Jan. 2013.
[33] R.-E. Precup, M.-B. Radac, R.-C. Roman, and E. M. Petriu, "Model-free sliding mode control of nonlinear systems: Algorithms and experiments," *Inf. Sci.*, vol. 381, pp. 176–192, Mar. 2017.
[34] T. D. Do, "Disturbance observer-based fuzzy SMC of WECSs without wind speed measurement," *IEEE Access*, vol. 5, pp. 147–155, 2016.
[35] D.-S. Liu, J. Li, and W.-S. Chang, "Internal model control for magnetic suspension system," in *Proc. Int. Conf. Mach. Learn. Cybern.*, vol. 1, Aug. 2005, pp. 482–487.
[36] H. K. Khalil, *Nonlinear Systems*, vol. 2. Upper Saddle River, NJ, USA: Prentice-Hall, 1996, pp. 1–5.
[37] R. Goodall, "On the robustness of flux feedback control for electromagnetic Maglev controllers," in *Proc. 16th Int. Conf. Magnetically-Levitated Syst. Linear Drives (MAGLEV)*, Rio de Janeiro, Brazil, Jun. 2000, pp. 197–202.
[38] W.-Q. Zhang, J. Li, K. Zhang, and P. Cui, "Measurement and control of magnetic flux signal in a maglev system," *Asian J. Control*, vol. 17, no. 1, pp. 165–175, 2015.
[39] J.-H. Li and J. Li, "A practical nonlinear controller for levitation system with magnetic flux feedback," *J. Central South Univ.*, vol. 23, no. 7, pp. 1729–1739, 2016.
[40] Y.-G. Li and W.-S. Chang, "Cascade control of an ems maglev vehicle's levitation control system," *Acta Automatica Sinica*, vol. 25, no. 2, pp. 247–251, 1999.
[41] A. Sakalli, T. Kumbasar, E. Yesil, and H. Hagras, "Analysis of the performances of type-1, self-tuning type-1 and interval type-2 fuzzy PID controllers on the Magnetic Levitation system," in *Proc. IEEE Int. Conf. Fuzzy Syst.*, Jul. 2014, pp. 1859–1866.
[42] J. Howell, "Aerodynamic response of maglev train models to a crosswind gust," *J. Wind Eng. Ind. Aerodyn.*, vol. 22, nos. 2–3, pp. 205–213, 1986.
[43] Y. Cai and S. Chen, "Numerical analysis for dynamic instability of electrodynamic maglev systems," *Shock Vib.*, vol. 2, no. 4, pp. 339–349, 1995.
[44] J.-H. Li, D.-F. Zhou, J. Li, G. Zhang, and P.-C. Yu, "Modeling and simulation of $CMS0_4$ maglev train with active controller," *J. Central South Univ.*, vol. 22, no. 4, pp. 1366–1377, 2015.

QIANG CHEN received the B.S. and M.S. degrees in automation from the National University of Defense Technology, Changsha, China, in 2012 and 2014, respectively, where he is currently pursuing the Ph.D. degree with the Maglev Engineering Center. His research interests include magnetic levitation control technologies and linear propulsion technologies.

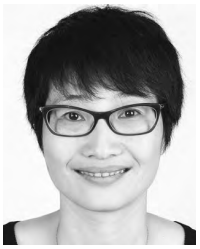

YING TAN received the Ph.D. degree in electrical engineering from the National University of Singapore in 2002. In 2002, she joined the Department of Chemical Engineering, McMaster University, as a Post-Doctoral Fellow. Since 2004, she has been with the Department of Electrical and Electronic Engineering, The University of Melbourne, where she is currently an Associate Professor and a Reader. Her current research interests are iterative learning control, extremum seeking control, nonlinear systems and applications in rehabilitation robotic systems, and engine operation optimizations.

JIE LI received the Ph.D. degree in automation from the National University of Defense Technology, Changsha, China, in 1999. He held a postdoctoral position with The Hong Kong University of Science and Technology, Hong Kong. He is currently a Professor with the Maglev Engineering Center, National University of Defense Technology. His research interests include the magnetic levitation technologies and robotics.

DENNY OETOMO received the B.Eng. degree (Hons.) from The Australian National University, Canberra, ACT, Australia, in 1997, and the Ph.D. degree from the National University of Singapore, Singapore, in 2004. He joined The University of Melbourne, Parkville, VIC, Australia, in 2008, where he is currently an Associate Professor. His current research interests include the manipulation strategies of robotics systems, with a focus on the biomedical and clinical applications.

IVEN MAREELS received the M.S. degree in electromechanical engineering from Ghent University, Belgium, in 1982, and the Ph.D. degree in systems engineering from The Australian National University, Canberra, Australia, in 1987. Since 1996, he has been a Professor of electrical and electronic engineering with the Department of Electrical and Electronic Engineering, The University of Melbourne. His current research interests are control and instrumentation for irrigation networks, control theory and automation, mathematical modeling of engineering systems, signal processing and data modeling, and systems engineering.